Food Hydrocolloids 135 (2023) 108121

Contents lists available at ScienceDirect

Food Hydrocolloids

journal homepage: www.elsevier.com/locate/foodhyd

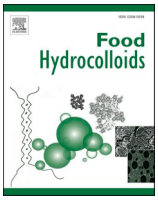

In vitro digestibility of O/W emulsions co-ingested with complex meals: Influence of the food matrix

Anna Molet-Rodríguez [a], Amelia Torcello-Gómez [b], Laura Salvia-Trujillo [a], Olga Martín-Belloso [a], Alan R. Mackie [b,*]

[a] Department of Food Technology, University of Lleida – Agrotecnio CERCA Center, Av. Alcalde Rovira Roure 191, 25198, Lleida, Spain
[b] School of Food Science & Nutrition, University of Leeds, Leeds, LS2 9JT, UK

ARTICLE INFO

Keywords:
Emulsions
β-carotene
Food matrix
Semi-dynamic digestion
Whole milk
Oatmeal

ABSTRACT

Oil-in-water (O/W) emulsions are promising delivery systems of lipophilic bioactive compounds into meals composed mainly of water. The colloidal stability of β-carotene-loaded O/W emulsion incorporated into whole milk, oatmeal and whole milk-oatmeal meals. Their subsequent gastric emptying rate, lipid digestibility and β-carotene retention during *in vitro* gastrointestinal digestion were evaluated using a semi-dynamic gastric model followed by a static small intestinal model. The dispersed particles within the meals, lipid droplets, casein micelles as well as protein and β-glucan aggregates, were responsible for the bigger average particle sizes of both O/W-oatmeal and O/W-whole milk-oatmeal (13.07 ± 1.81 and 7.60 ± 1.21 μm, respectively) compared to the O/W emulsions and O/W-whole milk (0.56 ± 0.03 and 0.44 ± 0.04 μm, respectively). Semi-dynamic *in vitro* gastric digestion of O/W-whole milk showed lipid droplets embedded into an insoluble protein network emptied earlier than the O/W emulsion. Conversely, O/W-oatmeal and O/W-whole milk-oatmeal had delayed lipid emptying, probably because of the gelation of the β-glucan from oats. During the *in vitro* small intestinal digestion, the rate of the FFA release was linked to the gastric emptying rate. Indeed, both O/W emulsion and O/W-whole milk presented an exponential increase in the FFA release, whereas the O/W-oatmeal and O/W-whole milk-oatmeal followed a stepwise trend. The β-carotene retention during *in vitro* gastrointestinal digestion depended on the lipid amount at each digestion time moment. Hence, this work provides valuable insight into the behaviour of O/W emulsions incorporated into meals and during their subsequent *in vitro* gastrointestinal digestion.

1. Introduction

The consumption of a diet rich in carotenoids, such as β-carotene, is well-known to have a positive impact on human health as they have been associated with functional properties, such as provitamin A activity, antioxidant capacity and enhancement of the immune system response (Maiani et al., 2009; Saini, Nile, & Park, 2015). Therefore, there is a growing interest in developing food products enriched with β-carotene to increase their functionality. Nevertheless, since β-carotene has a very low water solubility, its incorporation into water-based food matrices is limited (Saini et al., 2015). In addition, its susceptibility to chemical degradation in pH and temperature conditions like those found during gastrointestinal (GI) digestion, results in the loss of its functional properties (Boon, McClements, Weiss, & Decker, 2010). The use of oil-in-water (O/W) emulsions, consisting of dispersed oil droplets (from 100 nm to 10 μm) in a continuous aqueous phase, may facilitate the dispersion of β-carotene in water-based food matrices as well as its protection from degradation processes (Zhang et al., 2016). Nevertheless, there is very little information available regarding the colloidal stability of O/W emulsions once incorporated into high water content food matrices and during their passage through the different phases of GI digestion. Physicochemical properties of food macromolecules may be detrimental to O/W emulsions colloidal stability as they can interact with the oil droplet interface and/or modify the viscosity of the continuous phase (Gasa-Falcon, Odriozola-Serrano, Oms-Oliu, & Martín-Belloso, 2017; Thongngam & McClements, 2005). Moreover, the colloidal stability of O/W emulsions incorporated into food matrices is related to their subsequent gastric emptying rate, as well as lipid digestion rate and extent during small intestinal digestion. In addition, β-carotene may be oxidised, thus losing its functional properties upon GI conditions.

Semi-dynamic *in vitro* digestion models allow the behaviour of O/W

* Corresponding author.
E-mail address: A.R.Mackie@leeds.ac.uk (A.R. Mackie).

https://doi.org/10.1016/j.foodhyd.2022.108121
Received 4 May 2022; Received in revised form 31 August 2022; Accepted 3 September 2022
Available online 13 September 2022

emulsions or food matrices during gastric digestion to be simulated by adding acid, gastric fluids and enzymes gradually, as well as simulating the gastric emptying (GE) (Mulet-Cabero, 2020a). In fact, the behaviour of O/W emulsions or food matrices during gastric digestion using a semi-dynamic *in vitro* gastric model was previously assessed (Ferreira-Lazarte et al., 2017; Mulet-Cabero, Torcello-Gómez, et al., 2020; Mulet-Cabero, Mackie, Wilde, Fenelon, & Brodkorb, 2019). Nevertheless, to our knowledge, an understanding of O/W emulsions behaviour once co-digested with complex meals using a semi-dynamic *in vitro* gastric model is lacking.

Therefore, the aim of this work was to investigate the influence of food components, such as protein, lipid and fibre, on the colloidal stability of β-carotene-loaded O/W emulsions co-digested with complex meals before ingestion and throughout simulated GI digestion. To elucidate the real benefits of using O/W emulsions as delivery systems of β-carotene in complex meals, not only should the colloidal stability during *in vitro* GI digestion conditions be studied, but also their influence on emptying rate and lipid digestibility, as well as, β-carotene bioaccessibility. For this, β-carotene-loaded O/W emulsions stabilized with Tween 80 were incorporated into whole milk, oatmeal or whole milk-oatmeal and were submitted to a semi-dynamic *in vitro* gastric digestion. After simulating the oral phase, the meals containing the β-carotene-loaded O/W emulsion were submitted to a semi-dynamic *in vitro* gastric phase, with aliquots of the bolus taken after 5-time intervals, simulating the GE. The gastric chyme emptied at different times was then subjected to static *in vitro* small intestinal phase in order to evaluate lipid digestibility. The colloidal stability in terms of particle size, size distribution and microstructure of the meals containing the β-carotene-loaded O/W emulsion was determined before *in vitro* oral digestion and after the different gastric emptying times. Moreover, the β-carotene retention after the small intestinal phase of each gastric emptying (GE) was determined.

2. Material and methods

2.1. Material

Sunflower oil from a local supermarket (Tesco, Ireland), β-carotene (C9750) of ≥93% purity and polyoxyethylene-sorbitan monooleate (Tween 80) from Sigma Aldrich (St Louise, MO, USA) were the ingredients used in the formulation of the β-carotene-loaded O/W emulsion. Tween 80 was selected as emulsifier as it allows the formation of stable O/W emulsions with submicron particle size. Whole milk and Scottish oat flakes, used to prepare the meals in which the O/W emulsion was incorporated, were purchased from a local supermarket (Tesco, Ireland). α-amylase from human saliva (A1031), pepsin from porcine gastric mucosa (P7012), pancreatin from porcine pancreas (P7545) and bile extract porcine (B8631) were purchased from Sigma Aldrich (St Louise, MO, USA). The α-amylase activity reported by Sigma Aldrich was 97.80 U/mg solid. The activities of pepsin and pancreatin were measured according to the assays detailed in Brodkorb et al. (2019). Pepsin had an activity of 3940 U/mg solid and pancreatin had an activity of 6.48 U/mg solid. The fluorescence dyes, Nile red (N3013), fast green FCF (F7252) and methyl blue (95290), were purchased from Sigma Aldrich. The chemicals used in the extraction analysis to quantify the β-carotene concentration were ethanol absolute and hexane (fraction from petroleum), both HPLC grade (Sharlab S.L, Sentmenat, Spain). The rest of the chemicals used were of analytical grade. All solutions were prepared with milli-Q water with a resistivity of 18.2 MΩ cm at 25 °C (Milli-Q apparatus, Millipore, Bedford, UK).

2.2. Methods

2.2.1. Formulation of the β-carotene-loaded O/W emulsion and complex meals

2.2.1.1. Formation of the β-carotene-loaded O/W emulsion. Firstly, β-carotene was dispersed in sunflower oil (0.1 g/100 g) by sonicating (5 min) and heating (<50 °C, 10 min) three consecutive times, to obtain the lipid phase. Then, a coarse O/W emulsion was prepared by pre-homogenizing 20% (w/w) of lipid phase, Tween 80 (2% w/w) and milli-Q water (78% w/w) using a high shear laboratory mixer, T-25 digital Ultra-Turrax (IKA, Staufen, Germany), working at 7200 rpm for 3 min. An O/W emulsion with oil droplets in the submicron range was obtained by passing the coarse O/W emulsion two times through a Jet Homogenizer (a two-chamber homogenizer developed in the School of Food Science and Nutrition, University of Leeds, Leeds, UK) at a pressure of ~300 bar.

2.2.1.2. Formation of the complex meals. Three different meals, being whole milk, oatmeal and whole milk-oatmeal, were fortified with the O/W emulsion (O/W-meals). Oatmeal (*Avena sativa* L.) was chosen as a food matrix due to the rich β-glucan content, which has been suggested to have an impact on lipid digestibility (Grundy et al., 2017).

First, two preliminary blends were prepared by mixing (750 rpm; 5 min) the O/W emulsion (20% w/w) with 80% w/w of milli-Q water (O/W emulsion:water) or whole milk (O/W emulsion:whole milk), then, 87% (w/w) of the O/W emulsion:water or O/W emulsion:whole milk was diluted in milli-Q water (13% w/w) and subsequently, mixed and boiled (750 rpm; 5 min). These two systems are referred to in the manuscript as the O/W emulsion and O/W-whole milk. In addition, oat flakes were added to the O/W emulsion:water or O/W emulsion:whole milk to a final ratio of 13/87 and oatmeal was prepared by boiling and mixing at 750 rpm for 5 min. These two systems are referred in the manuscript as O/W-oatmeal and O/W-whole milk-oatmeal. Afterwards, they were allowed to cool down to room temperature before the *in vitro* GI digestion. Lipid, protein and fibre content, as well as the total solids of O/W emulsion and O/W-meals are listed in Table 1.

2.2.2. In vitro gastrointestinal digestion

The O/W emulsion and O/W-meals were submitted to simulated GI digestion. Oral and intestinal *in vitro* digestions were performed following the INFOGEST static protocol (Brodkorb et al., 2019). A semi-dynamic *in vitro* model recently described by Mulet-Cabero, Egger, et al. (2020) was used to mimic gastric digestion.

2.2.2.1. Stock solutions of simulated digestive fluids. The electrolyte stock solutions of digestion fluids (x1.25 concentrated), including electrolyte simulated salivary fluid (eSSF: KCl, KH_2PO_4, $NaHCO_3$, $MgCl_2(H_2O)_6$, $(NH_4)_2CO_3$, HCl), electrolyte simulated gastric fluid (eSGF: KCl, KH_2PO_4, $NaHCO_3$, NaCl, $MgCl_2(H_2O)_6$, $(NH_4)_2CO_3$) and electrolyte simulated intestinal fluid (eSIF: KCl, KH_2PO_4, NaCl, $MgCl_2(H_2O)_6$) were prepared according to Brodkorb et al. (2019), adjusted to pH 7 and stored at −20 °C. The authors of this method have stated that the use of carbonate salts in the electrolyte solutions requires the use of sealed containers with limited headspace. In open vessels, as in the case of the

Table 1
Compositional description of the β-carotene-loaded oil-in-water (O/W) emulsion and after incorporation into whole milk, oatmeal and whole milk-oatmeal.

Formulation	Lipid % (w/w)	Protein % (w/w)	Fibre % (w/w)	Total solids (g)
O/W emulsion	3.48	–	–	1.04
O/W-whole milk	6.06	2.44	3.27	3.53
O/W-oatmeal	4.39	1.34	7.87	4.08
O/W-whole mil-oatmeal	6.97	3.78	11.14	6.57

small intestine digestion of the present study, CO_2 would be released and the pH would progressively increase with time. Following their suggestions, in eSIF, sodium bicarbonate ($NaHCO_3$), the main source of carbonates, was replaced with NaCl at the same molar ratio to maintain the ionic strength of the electrolyte solutions.

2.2.2.2. Static in vitro oral digestion. In the reaction vessel, which was a v-form vessel (Yorlab, UK) with a thermostat jacket (37 °C), 30 g of O/W emulsion or O/W-meals were mixed with the oral mixture solution consisting of eSSF, $CaCl_2(H_2O)_2$ (0.3 M) and milli-Q water to a final ratio of 1:1 with the dry weight of food (Supplementary material Table S1). The volume of oral mixture solution added varied slightly between meals, ranging from 1.04 to 6.57 mL (Table 1 and Supplementary material Table S1). In addition, α-amylase (150 U/mL oral mixture solution) was added to the gastric mixture solution for the meals containing starch (O/W-oatmeal and O/W-whole milk-oatmeal). Then, the pH of the mixture was adjusted to 7 and incubated at 37 °C for 2 min with continuous agitation at 150 rpm using an overhead stirrer (Hei-TORQUE Value 100, Heidolph, Germany) with a 3D printed stirrer paddle.

2.2.2.3. Semi-dynamic in vitro gastric digestion. A gastric mixture solution was prepared to have a final ratio of 1:1 with the oral bolus. The gastric mixture solution consisted of SGF (eSGF, $CaCl_2(H_2O)_2$ (0.3 M) and milli-Q water), HCl (1 M) and pepsin solution (Supplementary material Table S2). The pH of the oral bolus was decreased to simulate the fasted state in the stomach by adding 10% of the SGF solution and HCl until reaching pH 2. During the gastric digestion, three solutions were added: (1) the remaining 90% of SGF solution at pH 7, (2) pepsin solution (4000 U/mL of gastric mixture solution) and (3) HCl (1 M). The volume of acid needed to decrease the pH of the tested O/W emulsion and O/W-meals to 2 was determined previously, following the pH test protocol described in Mulet-Cabero, Egger, et al. (2020). A dosing device (800 Dosino, Metrohm, Switzerland) with an automatic titrator (902 Titrando, Metrohm, Switzerland) was used to deliver both the gastric mixture solution and HCl. The enzyme solution was delivered by a syringe pump (Legato, Kd Scientific, USA). The rate at which these solutions were delivered was dependent on the total gastric digestion time of O/W emulsion or O/W-meals (Supplementary material Table S3 and S4). The gastric content was mixed at 10 rpm (using the same overhead stirrer as in the oral phase) and 37 °C during the total gastric phase time determined for each formulation.

The simulation of the GE was determined considering the composition of each fortified meal (Table 1) and calculating their caloric content (kcal/g of meal) based on the standard Atwater factors (1 g of lipid yields 9 kcal, 1 g of protein yields 4 kcal and 1 g of carbohydrates yields 4 kcal). The emptying rate used was constant and based on the caloric content of the studied meals and scaled-down from 2 kcal/min/mL of the realistic meal that would be digested *in vivo*, being 180 mL for the O/W emulsion and O/W-whole milk and 207 mL for the O/W-oatmeal and O/W-whole milk-oatmeal. Thus, the volume and time of each GE point differed between the fortified meals (Supplementary material Table S4). Gastric emptying was simulated by taking five aliquots, referred to as GE1-5 in the text, corresponding to the portion of O/W emulsion or O/W-meals that would be delivered into the duodenum. Aliquots were taken from the bottom of the vessel using a 10 mL pipette tip, the aperture of which had a 2 mm diameter because it approximates the upper limit of particle size that has been seen to pass through the pyloric opening into the duodenum (Thomas, 2006). To inhibit pepsin activity, NaOH (2 M) was added to each GE sample to increase the pH above 7. Aliquots of GEs were collected for immediate analysis of particle size and particle size distribution (GE1 and GE5) as well as confocal microscopy (GE1, GE3 and GE5) and the rest was snap-frozen in liquid nitrogen and stored at −80 °C for subsequent *in vitro* small intestinal digestion.

2.2.2.4. Static in vitro small intestinal digestion. Each GE was placed in a water bath at 37 °C and their *in vitro* small intestinal digestion (Brodkorb et al., 2019) was simulated using a pH-stat (Metrohm USA Inc., Riverview, FL, USA). The intestinal mixture was prepared using 42.5% (v/v) of eSIF, 0.2% (v/v) of $CaCl_2(H_2O)_2$ (0.3 M) and 19.8% (v/v) of Milli-Q water was added to each GE aliquot followed by an adjustment of pH to 7. Afterwards, 12.5% (v/v) of bile extract solution (20 mM in the intestinal mixture) and 25% (v/v) of pancreatin solution (200 U of trypsin/mL intestinal mixture) were also added. To compensate for the free fatty acids (FFAs) that were released during the lipid digestion, the pH was constantly maintained at 7 by adding dropwise a NaOH solution (0.25 M). After 120 min, the digest collected was transferred into a glass tube and heat-shocked at 85 °C for 5 min in order to stop the lipolysis reaction and placed in an iced-water bath afterwards. The volume of NaOH recorded during 120 min of small intestinal digestion of each GE was employed to calculate the lipid digestibility defined by the percentage of FFAs release, using equation (1) (Li & McClements, 2010):

$$\textit{Free fatty acids release}\ (\%) = \frac{V_{NaOH} \times C_{NaOH} \times M_{lipid}}{2 \times m_{lipid}} \times 100 \quad (1)$$

where V_{NaOH} is NaOH volume (mL) used to compensate the FFAs released during the digestion, C_{NaOH} is NaOH molarity (0.25 M), M_{lipid} is lipid molecular weight and m_{lipid} is lipid total weight present in the O/W emulsion or O/W-meals before starting the small intestinal digestion. The molecular weight was 872, 700 and 867 g/mol for sunflower oil, whole milk and oat flakes lipid, respectively. The m_{lipid} of the O/W emulsion, O/W-whole milk, O/W-oatmeal and O/W-whole milk-oatmeal was 0.95, 1.58, 1.15 and 1.84 g, respectively.

The percentage of FFA release of each GE aliquot of the O/W emulsion or O/W meals at the end of the small intestinal phase was calculated. Additionally, the accumulated FFA release of all the GE aliquots taken at different time moments was calculated as the sum of FFA release of each GE *versus* time in the small intestinal phase. The initial time of the small intestinal phase was considered as the beginning of the semi-dynamic gastric phase in order to account for the FFA release during 250 min, until all the aliquots of the GE completed the small intestinal *in vitro* digestion time. Moreover, the end-point total lipid digestibility was calculated as the sum of the FFAs release (%) in each individual GE.

2.2.3. Characterization of the β-carotene-loaded O/W emulsion and complex meals

Particle size, size distribution and confocal microscopy images were taken to determine structural changes that occurred once the O/W emulsion was incorporated in the studied meals and during their subsequent semi-dynamic *in vitro* gastric digestion, that is, in the GE aliquots.

2.2.3.1. Particle size and particle size distribution. Particle size and size distribution of initial (before *in vitro* oral digestion), GE1 and GE5 aliquots from O/W emulsion and O/W-meals were measured using static light scattering (SLS) (Mastersizer 2000, Malvern Instruments Ltd, Worcestershire, UK). Aliquots from O/W-oatmeal and O/W-whole milk-oatmeal were centrifuged at 3000 rpm for 5 min and the upper part was collected for its subsequent particle size measurement (Eppendorf 5702, Hamburg, Germany). Initial, GE1 and GE5 aliquots were diluted in milli-Q water and stirred in the dispersion unit with a speed of 2200 rpm. Particle size was reported as surface-weighted average ($D_{[3,2]}$) (data shown in the text) and size distribution as volume density (%). The refractive index of sunflower oil and water were 1.47 and 1.33, respectively.

2.2.3.2. Confocal laser scanning microscopy (CLSM). Confocal microscopy images of initial, GE1, GE3 and GE5 aliquots from O/W emulsion and O/W-meals were taken. A stock solution of Nile Red (1 mg/mL in

dimethyl sulfoxide) was used to stain the lipid, Fast Green (1 mg/mL in milli-Q water) was used to stain the protein and Methyl Blue (1 mg/mL in milli-Q water) was used to stain the β-glucan. Aliquots were dyed with the stock solutions of Nile red and Fast Green or Methyl blue and excited at wavelengths of 488, 633 and 665 nm, respectively. The emission filters were set at 555–620 nm for Nile Red, 660–710 nm for Fast Green and 550–700 nm for Methyl Blue. A Zeiss LSM 880 inverted confocal microscope (Carl Zeiss MicroImaging GmbH, Jena, Germany) with an oil immersion 63 × lens and the pinhole diameter maintained at 1 Airy Unit to filter out the majority of the scattered light was used to capture the confocal images. All images were processed using the instrument software Zen.

2.2.4. β-carotene retention after in vitro gastrointestinal digestion

The capacity of O/W emulsion and O/W-meals to retain β-carotene after being subjected to the prior described *in vitro* GI digestion was determined by the method reported by Liu, Wang, McClements, and Zou (2018) with minor modifications. A 1 mL-aliquot of the initial O/W emulsion or each GE digest was mixed with 1 mL of ethanol and 1.5 mL of hexane, vortexed for 10 s and centrifuged at 9000 rpm for 10 min at 4 °C (Universal 320R, Andreas Hettich GmbH & Co. KG, Tuttlingen, Germany). The hexane fraction was analyzed spectrophotometrically (CECIL CE 2021; Cecil Instruments Ltd, Cambridge, UK) at 450 nm. The concentration of β-carotene extracted from the initial O/W emulsion or each GE digest was determined from a calibration curve of absorbance versus β-carotene concentration in hexane. The β-carotene retention was then calculated using equation (2):

$$\beta - carotene\ retention(\%) = \frac{C_{digest}}{C_{initial}} \times 100 \quad (2)$$

where C_{digest} and $C_{initial}$ are the β-carotene concentration in each GE digest and in the initial O/W emulsion, respectively.

The total β-carotene retention of O/W emulsion or O/W-meals was calculated as the sum of the β-carotene retention in each of their individual GE samples after *in vitro* small intestinal digestion.

2.3. Statistical analysis

All experiments were assayed in duplicate and data was expressed as the mean with standard deviation. An analysis of variance was carried out and the Tukey HSD test was run to determine significant differences at a 5% significance level ($p < 0.05$) with statistical software JMP Pro 14 (SAS Institute Inc.).

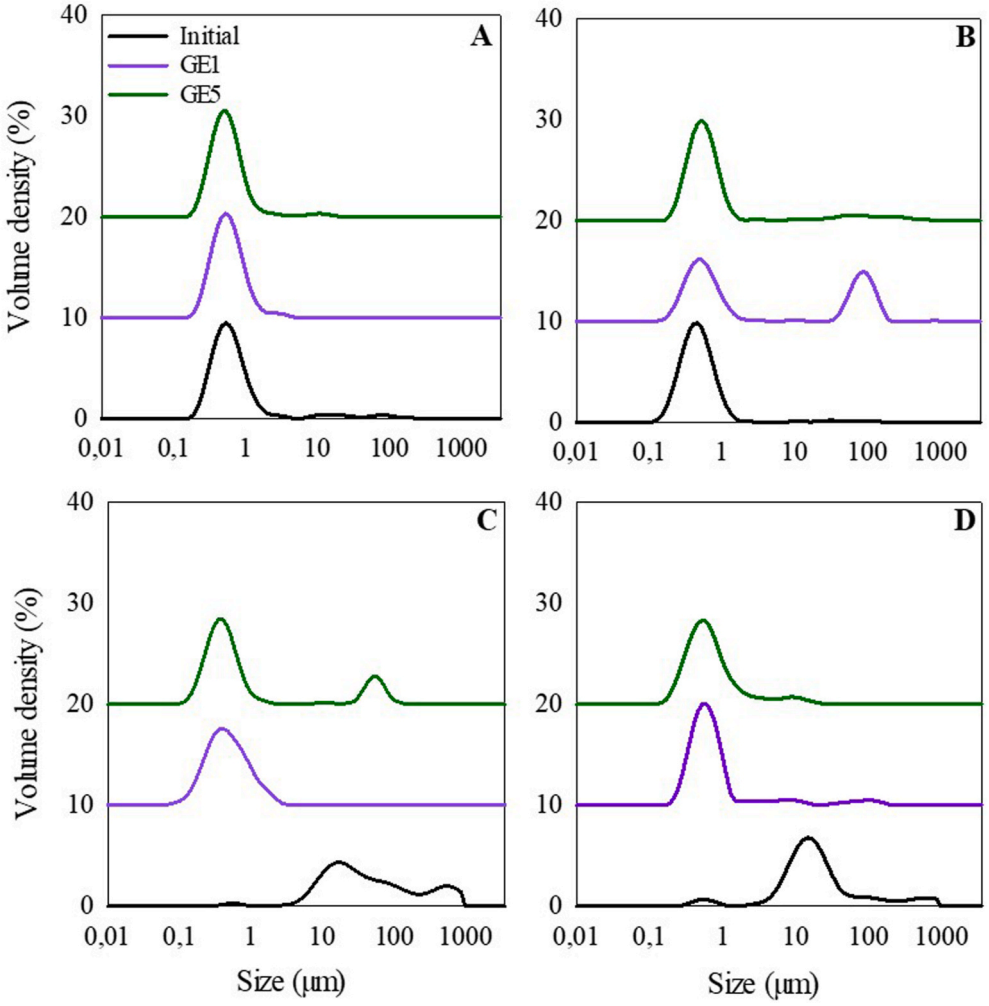

Fig. 1. Droplet size distribution in volume density (%) of the β-carotene-loaded oil-in-water (O/W) emulsion (A) and after incorporation into whole milk (B), oatmeal (C) and whole milk-oatmeal (D) initially (before *in vitro* oral digestion) and at gastric emptied (GE) aliquots 1 and 5 of the simulated *in vitro* gastric semi-dynamic digestion.

3. Results and discussion

3.1. Initial physicochemical properties of the β-carotene-loaded O/W emulsion and complex meals

Initial O/W emulsion had an average oil particle size of 0.56 ± 0.03 μm with a monomodal size distribution (Fig. 1A), and homogeneous dispersion of submicron oil droplets according to its initial CLSM image (Fig. 2). Incorporating the O/W emulsion into the studied complex meals resulted in submicron oil droplets from the O/W emulsion and colloidal particles from the meals co-dispersed in the aqueous phase (Fig. 2 and 3). In the case of the O/W-whole milk, its initial CLSM image clearly showed lipid (red) and protein (green) particles dispersed in the aqueous phase (Fig. 2). Lipid particles probably correspond to O/W emulsion oil droplets and milk fat globules, whereas protein particles were presumably casein micelles. Despite this, O/W-whole milk also presented submicron average particle size (0.44 ± 0.04 μm) and monomodal size distribution (Fig. 1B). Commercial whole milk is normally homogenized to reduce particle size (from 3 to 5 μm to below 1 μm) and increase the colloidal stability of native fat globules. In addition, it is well-known that casein micelles have particle sizes in the range of 50–500 nm (Fox & Brodkorb, 2008). In the present study, the reduced particle size of whole milk colloidal particles made it difficult to distinguish between them and submicron oil droplets from O/W emulsion by light scattering, thus observing no differences in the average particle size and size distribution of O/W emulsion and O/W-whole milk. Regarding O/W-oatmeal and O/W-whole milk-oatmeal, they presented significantly larger initial average particle sizes (13.07 ± 1.81 and 7.60 ± 1.21 μm, respectively) than O/W-whole milk, which correlated with the existence of particle populations in the micro-range in the particle size distribution graph (Fig. 1C and D). In this regard, CLSM images of both oatmeal and whole milk-oatmeal (without O/W emulsion) evidenced large lipid particles, as well as clusters of β-glucan (blue) and/or protein (green) (Supplementary material, Fig. S1). Thus, the microstructure of oatmeal and whole milk-oatmeal would be responsible for the larger average particle sizes and size distributions observed in the O/W-oatmeal and O/W-whole milk-oatmeal compared to the O/W-whole milk. Oat flakes are good sources of β-glucan fibre, which is a linear unbranched polysaccharide composed of consecutive β-D-glucopyranosyl units linked by β(1–3) and β(1–4) glycosidic bonds (White, Fisk, & Gray, 2006). On the one hand, repeated units of three (cellotriosyl) or four (cellotetraosyl) sequences separated by single β(1–3) linkages in the polysaccharide chain are known to favour auto-aggregation through hydrogen bonds, explaining the observed

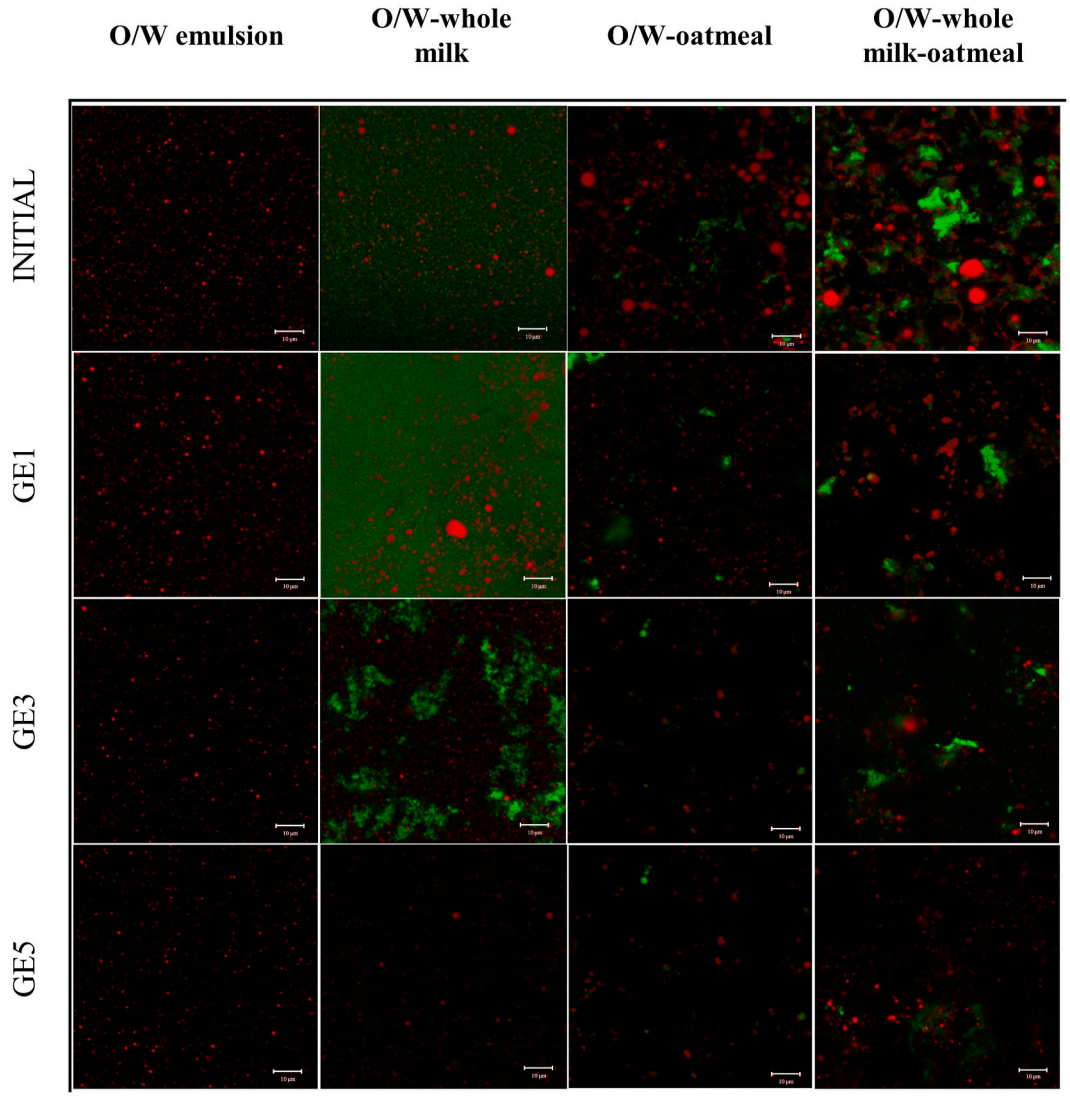

Fig. 2. Confocal microscopy images of the β-carotene-loaded oil-in-water (O/W) emulsion and after incorporation into whole milk, oatmeal and whole milk-oatmeal initially (before *in vitro* oral digestion) and at gastric emptied (GE) aliquots 1, 3 and 5 of the semi-dynamic *in vitro* gastric digestion. Protein and lipid in green (dye: Fast Green) and red (dye: Nile Red), respectively. The scale bar corresponds to 10 μm.

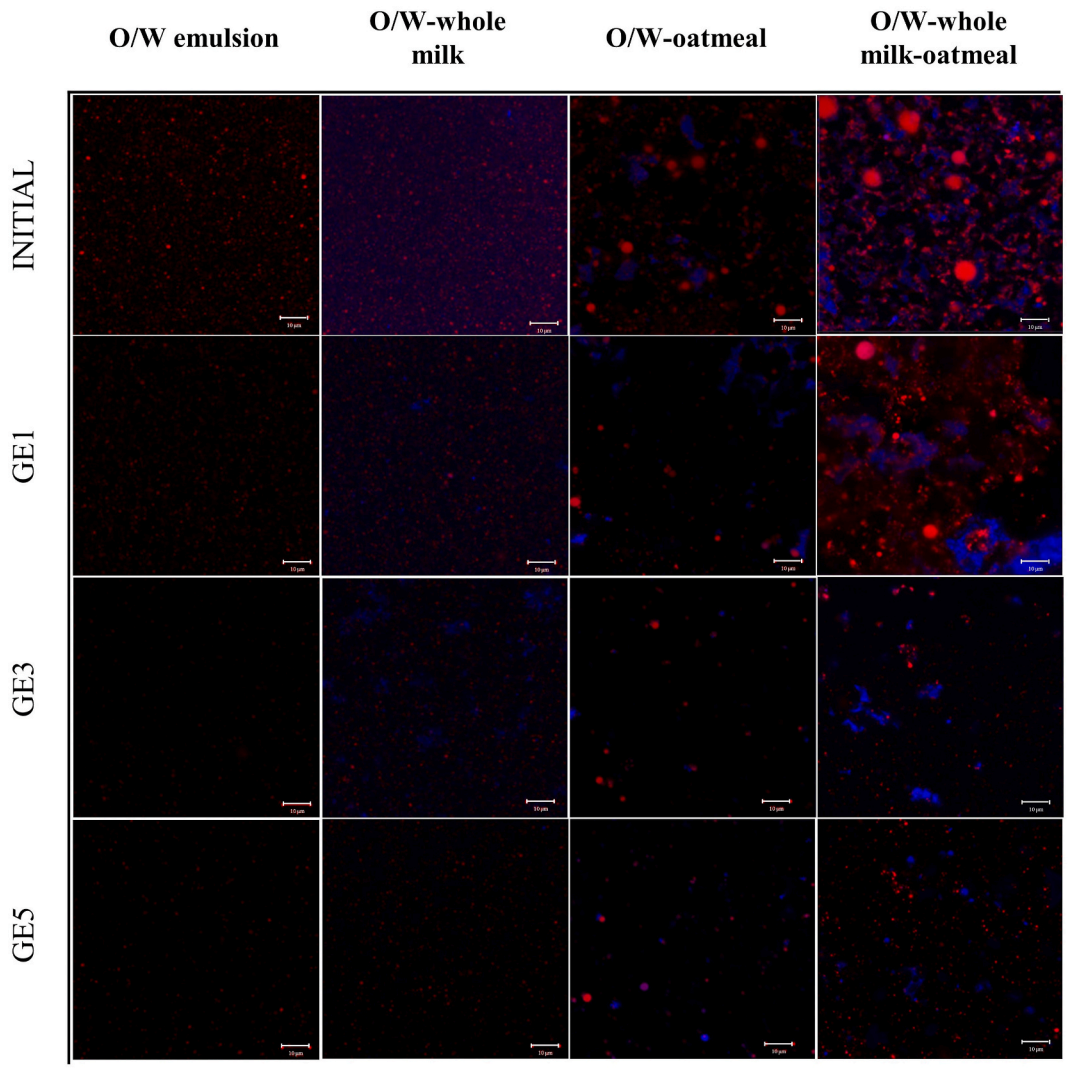

Fig. 3. Confocal microscopy images of the β-carotene-loaded oil-in-water (O/W) emulsion and after incorporation into whole milk, oatmeal and whole milk-oatmeal initially (before *in vitro* oral digestion) and at gastric emptied (GE) aliquots 1, 3 and 5 of the semi-dynamic *in vitro* gastric digestion. β-glucan and lipid in blue (dye: Methyl blue) and red (dye: Nile Red), respectively. The scale bar corresponds to 10 μm.

β-glucan aggregates and the higher particle size of O/W-oatmeal and O/W-whole milk-oatmeal compared to O/W emulsion and O/W-whole milk (Tosh, Brummer, Wood, Wang, & Weisz, 2004; Wu et al., 2006). On the other hand, studies on the stability of casein micelles in contact with β-glucan have demonstrated limited compatibility between them (De Bont, Van Kempen, & Vreeker, 2002; Goh, Sarkar, & Singh, 2014). In particular, these authors have stated that the exclusion of β-glucan from the surface area of casein micelles may cause osmotic attraction of casein micelles and consequently their aggregation. In agreement with this, in the present study, aggregates of protein were observed in the CLSM image of the O/W-whole milk-oatmeal (Fig. 2).

Despite the microstructure of the O/W emulsion and the complex meals, differences were also observed in their initial visual appearance, which showed that both O/W-oatmeal and O/W-whole milk-oatmeal had a gel-like appearance, while the O/W emulsion and O/W-whole milk were liquid (Fig. 4).

3.2. *In vitro gastrointestinal digestion of the β-carotene-loaded O/W emulsion and complex meals*

3.2.1. *Semi-dynamic in vitro gastric digestion*

During semi-dynamic *in vitro* gastric digestion, O/W emulsion or O/W-meals were mixed with gastric fluids containing pepsin and HCl. As a consequence of this acidification, meal microstructure could be altered due to protein precipitation and the formation of aggregates (Francis, Glover, Yu, Povey, & Holmes, 2019). In addition, gastric samples were taken after 5-time intervals, simulating GE. Hence, changes in both the gastric pH and meal microstructure in each GE aliquot will be discussed in the following sections.

3.2.1.1. Gastric pH. Before the gastric digestion, the gastric mixture showed pH values of 2, simulating the fasted state (Fig. 5A and B). Once the O/W emulsion or O/W-meals were added to the reaction vessel, the pH increased to around 6 due to the buffering capacity of some of their components (Salaün, Mietton, & Gaucheron, 2005). During gastric digestion, this pH decreased back to the basal conditions due to both the addition of HCl and the emptying of nutrients with buffering capacity to the subsequent static small intestinal phase (Mulet-Cabero, Egger, et al., 2020). Nevertheless, significant differences in pH at the initial stages of gastric digestion (GE1 and GE2) were observed between the tested formulations. In particular, after GE1 time of gastric digestion, the O/W emulsion had a pH of 2.07 ± 0.20, that is to say, it rapidly reached the basal pH. Contrarily, the gastric pH of the O/W-whole milk, O/W-oatmeal and O/W-whole milk-oatmeal at the same emptying point was 5.19 ± 0.006, 2.92 ± 0.24 and 3.95 ± 0.23, respectively (Fig. 5A). Thus, the incorporation of milk with the O/W emulsion led to higher

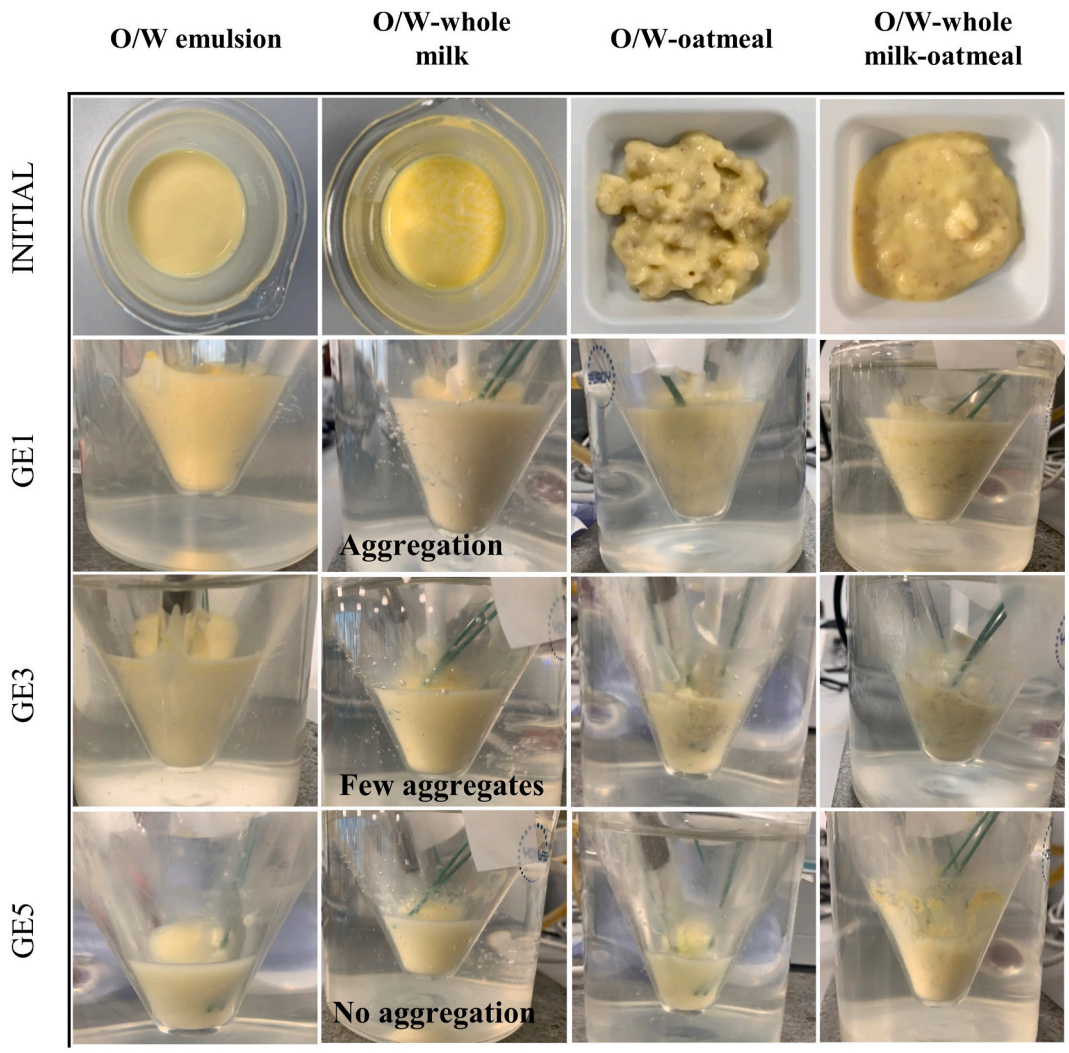

Fig. 4. Visual appearance of the β-carotene-loaded oil-in-water (O/W) emulsion and after incorporation into whole milk, oatmeal and whole milk-oatmeal initially (before *in vitro* = oral digestion) and at gastric emptying (GE) time points 1, 3 and 5 of *in vitro* gastric semi-dynamic digestion.

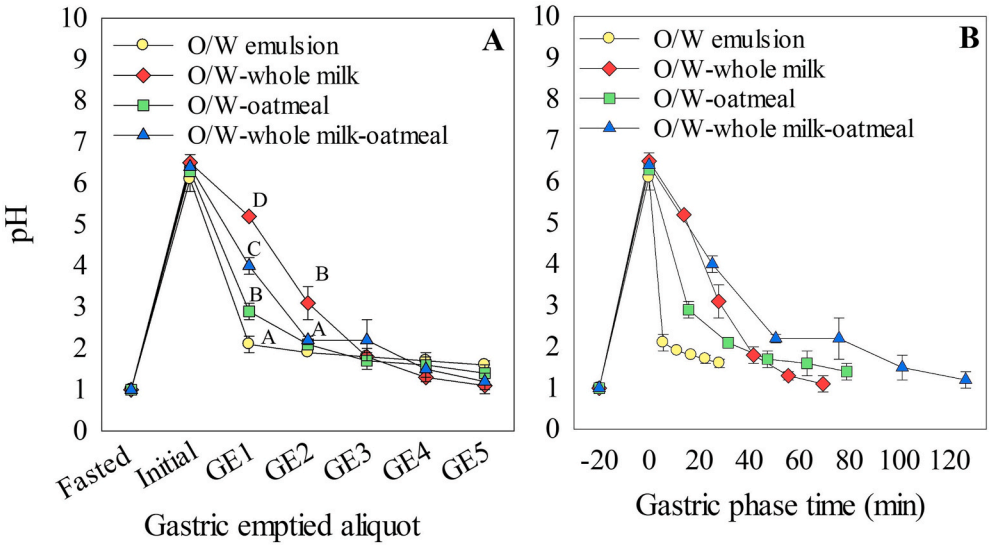

Fig. 5. Gastric pH changes of the β-carotene-loaded oil-in-water (O/W) emulsion (○) and after incorporation into whole milk (◊), oatmeal (□) and whole milk-oatmeal (Δ) during semi-dynamic *in vitro* gastric digestion, expressed as function of gastric emptying (GE) points (A) and as function of the digestion time (B). Fasted state (before gastric digestion), initial (meals including oral phase and basal volume) and GE aliquots (GE1-GE5), food taken form the gastric bolus at different time moments..

resistance to pH changes upon gastric acid addition. In this sense, it is well-known that, in foods, buffering capacity is primarily influenced by protein, which has the ability to act as a buffer (Mennah-Govela & Bornhorst, 2021). For instance, acidic amino acids present in protein (*e.g.* aspartic and glutamic acids) have the ability to resist the changes of the gastric pH by neutralizing the H^+ added to the vessel (Mennah-Govela, Singh, & Bornhorst, 2019). In addition, a recent study dealing with the buffering capacity of several protein-based model food systems have reported a much higher buffering capacity in those food models with higher protein content (Mennah-Govela et al., 2019). In this context, pH differences in GE1 between O/W-whole milk and O/W-oatmeal might be attributed to the higher protein content in whole milk (2.44% w/w) in comparison with oatmeal (1.34% w/w) (Table 1). Nevertheless, even though the O/W-whole milk-oatmeal contained the highest protein content (3.78% w/w), it exhibited lower pH values in GE1 than the O/W-whole milk. The lower buffering capacity of the O/W-whole milk-oatmeal compared to O/W-whole milk might have been caused by the previously mentioned casein aggregation due to the presence of β-glucan (see section 3.1). In O/W-whole milk-oatmeal, aggregation of casein micelles induced by the presence of β-glucan might have led to the reduction of exposed acidic amino acid groups located in the surface, explaining its lower buffering capacity in comparison with the O/W-whole milk (Francis et al., 2019; Mennah-Govela & Bornhorst, 2021). The same tendency was observed at subsequent gastric digestion time points (GE2), with the O/W-whole milk presenting significantly higher pH compared to the other studied meals fortified with O/W emulsion. From GE3 until the end of the gastric digestion (GE5), all the O/W-meals reached the basal pH without statistically significant differences among them, which might be due to a reduction of the buffering capacity in advanced gastric digestion times. This was confirmed by the CLSM images of all O/W-meals in GE3 and GE5 (Fig. 2), which showed low protein content, presumably because of its earlier emptying.

3.2.1.2. Microstructural changes. The particle size distribution of the O/W emulsion in GE1 and GE5 was not significantly different from the initial one, showing that it remained stable during its passage through gastric digestion (Fig. 1A). In contrast, the particle size distribution of the studied O/W-meals varied during the gastric digestion time due to pH changes and/or proteolysis occurring during gastric digestion (Fig. 1B, C and D).The initial monomodal distribution observed for the O/W-whole milk became multimodal in GE1. It presented one peak in the submicron range, which may belong to O/W emulsion oil droplets, milk fat globules and casein micelles, and another around 114 μm. This population of bigger droplets could correspond to the network of aggregated protein observed by CLSM in GE1 (Fig. 2). Casein micelles at pH close to their isoelectric point (pH 4.5–4.7) are known to precipitate (Francis et al., 2019). However, GE1 of O/W-whole milk had higher pH (5.19 ± 0.006) than the pI of caseins (Fig. 5A). Thus, other factors might also have caused the aggregation of casein molecules in GE1. In fact, it has been previously reported that pepsin favours the hydrolysis of κ-caseins, which leads to a reduction of the steric repulsion between casein micelles and consequently their aggregation at higher pH values than the casein pI (Mulet-Cabero, Torcello-Gómez, et al., 2020; Tam & Whitaker, 1972). Nevertheless, the size distribution of O/W-whole milk in GE5 was monomodal again, which could be explained by an absence of protein in this GE aliquot because of its earlier emptying (Fig. 1B). This was confirmed by CLSM images that showed the presence of protein molecules in all the GE aliquots except in GE5 (Fig. 2). On the other hand, the initial multimodal distributions of the O/W-oatmeal and O/W-whole milk-oatmeal, which were attributed to the protein and β-glucan aggregates from meal matrices, became monomodal in GE1 (Fig. 1C and D). This could be due to the re-dissolution of protein and β-glucan aggregates by the secretion of gastric fluids during the gastric digestion time (Fig. 2 and 3). In GE5, O/W-oatmeal presented a multimodal size distribution with one population of particles in the submicron range and another between 10 and 100 μm. Instead, O/W-whole milk-oatmeal size distribution was monomodal. The population of micrometric particles in O/W-oatmeal could be explained by the re-aggregation of β-glucan in GE5 because of the increase in the ionic strength by SGF (Sarantis, Eren, Kowalcyk, Jimenez–Flores, & Alvarez, 2021). Nevertheless, the re-aggregation of β-glucan due to the increase in the ionic strength would not occur in presence of milk protein as observed in O/W-whole milk oatmeal.

3.2.2. Static in vitro small intestinal digestion

3.2.2.1. Lipid digestibility during the in vitro small intestinal digestion. The accumulated FFA release percentage of the O/W emulsion or O/W-meals during 250 min of the *in vitro* small intestinal digestion is related to the lipid content of the formulations at different digestion times and therefore to their gastric emptying rate (Fig. 6). In general, they presented an increase in the FFA release values during digestion time until they reached a maximum FFA release between 120 and 150 min of digestion. This peak corresponds to the end of the small intestinal digestion of GE1. After this point, the FFA release continued but at a decreased rate, which might be attributed to the digestion of the subsequent GE aliquots, which were more diluted due to the addition of gastric fluids. Nevertheless, there were differences in the FFA release percentages among the O/W emulsion and the different complex meals during the first 150 min of small intestinal digestion. The O/W emulsion presented an exponential increase in the FFA release, subsequently followed by a steady-state zone until complete lipid digestion around 125 min. The O/W-whole milk followed a similar trend, but with higher FFA values due to their higher absolute lipid content. In contrast, both O/W-oatmeal and O/W-whole milk-oatmeal showed an increase of the FFA release following a stepwise trend, yet with differences among them. This suggests higher gastric retention in both O/W-oatmeal and O/W-whole milk-oatmeal compared to O/W emulsion and O/W-whole milk, which might be attributed to the physicochemical properties of the oat flakes. Similarly, other authors have also reported increased gastric retention of semi-solid meals compared to liquid ones due to their elevated viscosity (Mackie, Rafiee, Malcolm, Salt, & van Aken, 2013). In the present study, the β-glucan within oat flakes could have possibly altered the physicochemical properties of the food systems by either increasing their viscosity and/or forming a gel depending on their molecular weight. Thus, explaining the delay in the lipid emptying observed when the O/W emulsion was incorporated in meals containing oat flakes (Brummer et al., 2014; Regand, Tosh, Wolever, & Wood, 2009; Tosh et al., 2004). This was confirmed by the presence of solubilized β-glucan in the aqueous phase of O/W-oatmeal and O/W-whole milk-oatmeal along the gastric digestion time, as observed in their CLSM images (Fig. 3). In addition, as mentioned previously (see section 3.1), both O/W-oatmeal and O/W-whole milk-oatmeal had a gel-like appearance, thus corroborating their higher viscosity compared to the O/W emulsion and O/W-whole milk, which had a liquid appearance (Fig. 4).

The *in vitro* lipid digestibility at the end of the small intestinal phase of each GE, measured as the end-point value of the FFA release, is also related to the lipid content of the samples taken at different gastric digestion moments (Fig. 7). In this regard, O/W emulsion showed a gradual decrease in FFA release along the different GEs, from 14.0074 ± 1.7979 (GE1) to 7.2041 ± 1.5711% (GE5). This can be related to the dilution that occurs during the gastric phase, subsequently decreasing the concentration of lipids in the gastric vessel over time. Hence, O/W emulsion at GE1 presented a higher oil concentration than at GE2, and it decreased progressively in subsequent GE points. This suggests that the O/W emulsion presents high colloidal stability in the gastric phase, as seen in CLSM images (Fig. 2) since the dilution factor during the gastric phase determines the lipid digestibility in the small intestinal phase. In fact, it has been widely reported that Tween 80 renders highly stable

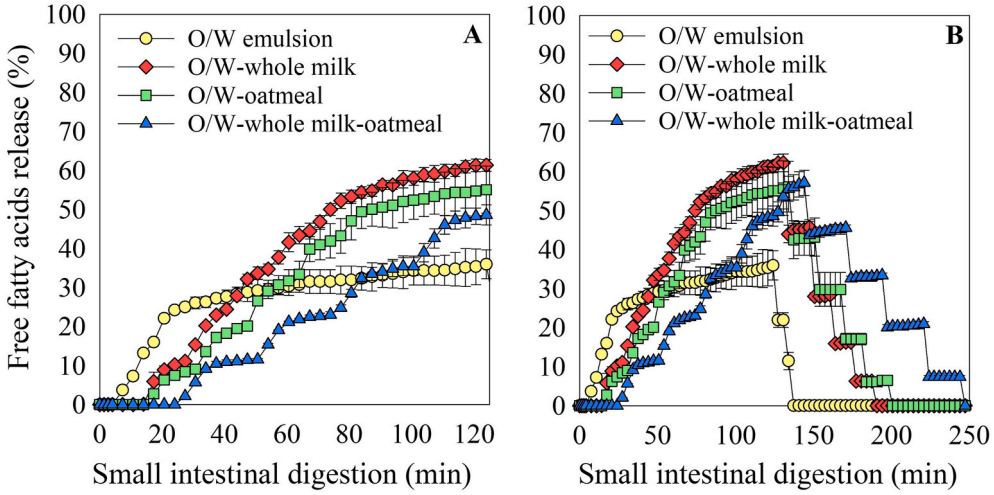

Fig. 6. Lipid digestibility of the β-carotene oil-in-water (O/W) emulsion (○) and after incorporation into whole milk (◇), oatmeal (□) and whole milk-oatmeal (Δ) during 125 min (A) and 250 min (B) of *in vitro* small intestinal digestion, expressed as the accumulated percentage of free fatty acid release of the different gastric emptying. .

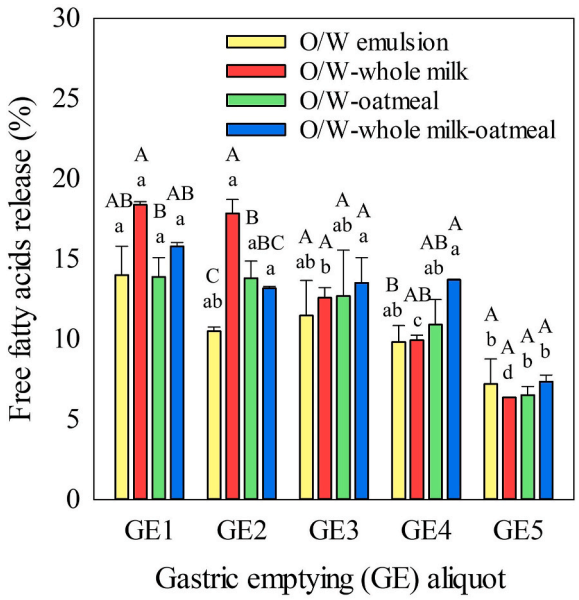

Fig. 7. Lipid digestibility of the different gastric emptying (GE), aliquots taken form the gastric bolus at different time moments, from the β-carotene-loaded oil-in-water (O/W) emulsion (yellow) and after incorporation into whole milk (red), oatmeal (green) and whole milk-oatmeal (blue) at the end of *in vitro* small intestinal digestion expressed as the percentage of free fatty acid release. Different upper-case letters mean significant differences between formulations for the same GE. Different lower-case letters indicate significant differences between GE aliquots for the same formulation.

emulsions under gastric conditions, in contrast with other surfactants (Verkempinck et al., 2018). In this sense, other authors have reported a gradual decrease in FFA release along with the gastric emptying of O/W emulsions when subjected to semi-dynamic *in vitro* digestion and a sudden increase at the final GE, which is attributed to the emptying of the creamed lipid layer of unstable emulsions (Mulet-Cabero, Torcello-Gómez, et al., 2020). Hence, the FFA release in the small intestine after the semi-dynamic gastric phase may not only indicate the amount of lipid that is delivered into the small intestinal phase but also may be related to the stability of the O/W emulsion under gastric conditions when incorporated into different meals. For instance, the gradual decrease in FFA release from GE1 to GE2 for the O/W emulsion was not observed for the O/W-whole milk. In fact, similar FFA release was observed in both GE1 (18.39 ± 0.20%) and GE2 (17.85 ± 0.87%) of O/W-whole milk, showing that the presence of whole milk led to a greater amount of lipid emptied at early times of the gastric digestion in comparison with the O/W emulsion (Fig. 7). CLSM images of the O/W-whole milk at GE1 showed lipid droplets entrapped in a network of protein formed by their precipitation due to the action of pepsin (see section 3.2.1.2) (Fig. 2). Hence, the larger amount of lipid in GE1 and GE2 of O/W-whole milk could be explained by the migration of the protein network to the bottom of the vessel (sedimentation), thus emptying the lipid droplets entrapped in the protein network at early gastric times (GE1 and GE2) (Mulet-Cabero et al., 2019). In the subsequent GE samples, FFA release percentage decreased gradually from 12.60 ± 0.63 (GE3) to 6.37 ± 0.03% (GE5), thus behaving as the O/W emulsions (Fig. 7). This behaviour could be attributed to the low protein content present in these GE samples, as observed in the CLSM images of GE3 and GE5. Regarding the O/W-whole milk-oatmeal, it presented a lower FFA release percentage at GE1 (15.80 ± 0.24%) than the O/W-whole milk (18.39 ± 0.20%), even though having a larger amount of lipid initially (Fig. 7 and Table 1). In addition, it is important to notice that FFA release percentages in GE aliquots 1 to 4 of O/W-oatmeal and O/W-whole milk-oatmeal remained practically constant and decreased at GE5 (Fig. 7). For instance, O/W-whole milk-oatmeal between GE1 and GE4 presented end-point FFA release values from 15.80 to 13.71%, whereas it was 7.36 ± 0.42% in GE5. Thus, it corroborated that the oat flakes-containing matrices slow down the emptying of the lipid from the gastric to the small intestinal phase because of the already mentioned higher viscosity of these meals compared to whole milk.

3.2.2.2. Total lipid digestibility of β-carotene-loaded O/W emulsion and complex meals. The total lipid digestibility of O/W emulsion at the end of the *in vitro* small intestinal digestion, measured as the total percentage

Table 2
Total lipid digestibility of the β-carotene-loaded oil-in-water emulsion (O/W) and after incorporation into whole milk, oatmeal and whole milk-oatmeal at the end of the *in vitro* small intestinal digestion, expressed as the percentage of free fatty acids release.

Formulation	Total free fatty acid release (%)
O/W emulsion	53.04 ± 6.33^{A}
O/W-whole milk	65.16 ± 2.03^{A}
O/W-oatmeal	57.85 ± 6.13^{A}
O/W-whole milk-oatmeal	63.57 ± 0.73^{A}

of FFA release, was 53.04 ± 6.33% (Table 2). The incomplete lipid digestion could be attributed to the fatty acid chain-length of the triglyceride oil used to formulate the O/W emulsion. It has been previously reported that long-chain triglyceride (LCT) oil, like sunflower oil, tend to accumulate at the oil/water interface, thus hindering lipase activity (Li, Hu, & McClements, 2011). The lipid digestibility of O/W-whole milk (65.16 ± 2.03%), O/W-oatmeal (57.85 ± 6.13%) and O/W-whole milk-oatmeal (63.57 ± 0.73%) tended to be greater compared to the O/W emulsion, although no significant differences were observed between them (Table 2). One possible explanation for this increase is that milk fat globules may have demonstrated a larger extent of hydrolysis in comparison with sunflower oil droplets from the O/W emulsion. Triglycerides consist of a glycerol molecule having three fatty acids esterified at the hydroxyl residues, one in the central position of the glycerol molecule (sn-2) and the other two at the terminal positions sn-1 and sn-3. It has been accepted that fatty acids on sn-2 carbon have greater bond energy and are more difficult to be lost than those at sn-1 and sn-3 positions (Karupaiah & Sundram, 2007). Whole milk contains substantial quantities of short and medium-chain fatty acids (C_4–C_{10}), which predominantly occupy the primary positions of the acylglycerol (sn-1 and sn-3) (Lubary, Hofland, & ter Horst, 2011). In turn, sunflower oil is mostly composed of long-chain fatty acids ($\geq C_{12}$), such as linoleic and oleic, that are mainly esterified in sn-2 and sn-3, respectively (Gao et al., 2017; Timm-Heinrich, Xu, Nielsen, & Jacobsen, 2003). Medium- (MCT) and short-chain triglycerides (SCT) are known to be digested by lipase more rapidly than LCT, which might be related to a greater digestibility of the milk fat in comparison with the oil droplets (Salvia--Trujillo, Qian, Martín-Belloso, & McClements, 2013).

3.3. β-carotene retention after in vitro gastrointestinal digestion of the O/W emulsion and complex meals

The concentration of β-carotene in each GE sample after the *in vitro* small intestinal digestion of the O/W emulsion or O/W-meals was determined, and the percentage of β-carotene retained was calculated based on its initial concentration in O/W emulsion. In general, as gastric digestion progressed (from GE1 to GE5), the β-carotene retention tended to decrease, although no significant differences were observed (Fig. 8). The total β-carotene retention at the end of the small intestinal digestion of the O/W emulsion was 15.48 ± 8.40% (Table 3). Due to its unsaturated structure, β-carotene is highly susceptible to degradation during digestion. However, the incorporation of β-carotene into emulsions is known to reduce its degradation even when exposed to environmental stresses such as the pH and temperature of the digestion process (Mao et al., 2009). In fact, other authors have reported β-carotene retention values above 50% after *in vitro* digestion of O/W emulsions of similar droplet size (Liu et al., 2018). The differences between the results observed in the present work and previously reported data may rely on the surfactant used to stabilize the oil/water interface. In fact, several authors reported that β-carotene degradation in Tween-stabilized O/W emulsions was significantly faster than in protein-stabilized ones, which might be explained by several reasons (Jo & Kwon, 2014; Mao et al., 2009; Qian, Decker, Xiao, & McClements, 2012). First, protein-stabilized O/W emulsions have more negatively charged oil droplets than Tween-stabilized ones, favouring their repulsion. Second, milk protein is known to have antioxidant properties due to its ability to scavenge free radicals and chelate pro-oxidant transition metals, avoiding β-carotene oxidation. Thirdly, it has been suggested that protein forms relatively thicker interfacial layers than Tween around lipid droplets acting as a physical barrier that separated the lipophilic bioactive compound from the aqueous phase pro-oxidants. In addition, the macromolecules present in each meal affected the total β-carotene retention, which was 26.35 ± 9.07, 28.53 ± 4.61 and 20.20 ± 3.51% for O/W-whole milk, O/W-oatmeal and O/W-whole milk-oatmeal, respectively (Table 3). This fact has also been observed by other researchers, who hypothesized that enhanced protection of β-carotene encapsulated in O/W emulsions incorporated in milk in comparison with water can be explained by the presence of protein and polysaccharide in these food systems (Chuacharoen & Sabliov, 2016). Other authors have stated that polysaccharides are capable of retarding carotenoid oxidation in O/W emulsions by *(i)* slowing down the diffusion of prooxidants to oil droplet surface because of the viscosity increase and *(ii)* metal ion chelation and hydrogen donation, through which polysaccharides function as radical chain breakers (Sun, Gunasekaran, & Richards, 2007).

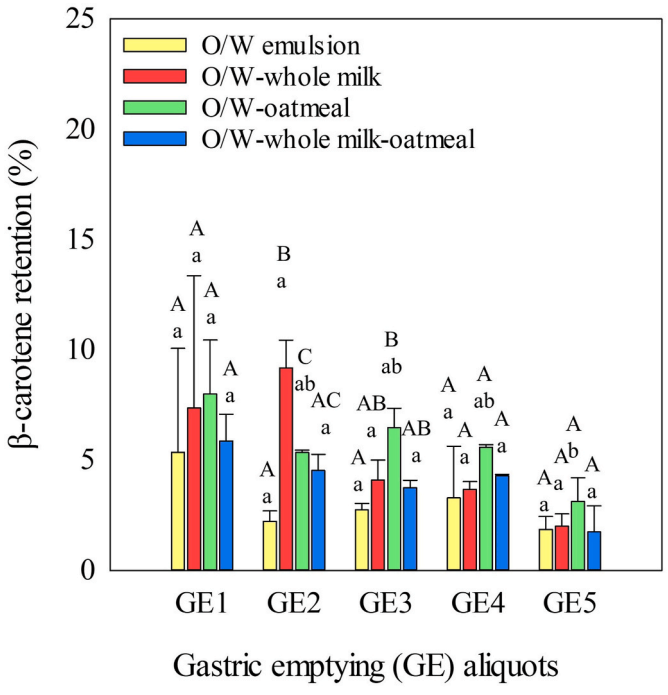

Fig. 8. β-carotene retention (%) after *in vitro* gastrointestinal digestion of the different gastric emptying (GE), aliquots taken form the gastric bolus at different time moments,from the β-carotene O/W emulsion (yellow) and after incorporation into whole milk (red), oatmeal (green) and whole milk-oatmeal (blue). Different upper-case letters mean significant differences between formulations for the same GE. Different lower-case letters indicate significant differences between GE aliquots for the same formulation.

4. Conclusions

The present study provides useful information about the influence of food matrix components, such as protein and lipid, and fibre, on the colloidal stability of β-carotene-loaded O/W emulsions once incorporated into complex meals. Data was measured on their subsequent colloidal stability, lipid emptying rate, lipid digestibility and β-carotene retention throughout a semi-dynamic *in vitro* gastric digestion model and subsequent static small intestine model. The particle size of the O/W emulsion incorporated into a meal consisting of a combination of milk and oat flakes was determined by the limited compatibility between casein micelles and β-glucan, which translated into bigger particle sizes than the O/W emulsion. During semi-dynamic *in vitro* gastric digestion,

Table 3
Total β-carotene retained (%) after *in vitro* gastrointestinal digestion of the oil-in-water (O/W) emulsion and after incorporation into whole milk, oatmeal and whole milk-oatmeal.

Formulation	Total β-carotene retained (%)
O/W emulsion	15.48 ± 8.40^{A}
O/W-whole milk	26.35 ± 9.07^{A}
O/W-oatmeal	28.53 ± 4.61^{A}
O/W-whole milk-oatmeal	20.20 ± 3.51^{A}

it was evident that microstructural changes of meal matrices as a result of macromolecule interactions influenced the lipid emptying rate. Casein precipitation during the gastric phase led to a faster lipid emptying for the O/W-whole milk than the O/W emulsion, whereas it was delayed in both O/W-oatmeal and O/W-whole milk-oatmeal probably due to viscosity increase by the presence of β-glucan. Accordingly, during *in vitro* small intestinal digestion, O/W emulsion and O/W-whole milk showed an exponential increase in the FFA release, whereas in the case of the oatmeal-containing meals (O/W-oatmeal and O/W-whole milk-oatmeal) the increase in the FFA values followed a step-wise trend. Apart from that, O/W-whole milk presented the highest total lipid digestibility, probably due to the faster and more extensive digestion of milk fat globules compared to O/W emulsion oil droplets, although there were no significant differences. Finally, β-carotene retention during the GI digestion was linked to the amount of lipid being emptied at each time point. In addition, milk and oat flakes components could be protecting β-carotene against degradation, since the incorporation of the O/W emulsions into complex meals tended to increase the retention of β-carotene after the *in vitro* small intestinal digestion. Hence, this work elucidates the contribution of whole milk and/or oat flakes within complex food matrices, to the formation and digestibility of meals fortified with O/W emulsions as carriers of lipophilic bioactive compounds.

CRediT authorship contribution statement

Anna Molet-Rodríguez: Conceptualization, Methodology, Formal analysis, Investigation, Visualization, Writing – original draft. **Amelia Torcello-Gómez:** Conceptualization, Methodology, Visualization, Resources, Writing – review & editing. **Laura Salvia-Trujillo:** Formal analysis, Visualization, Supervision, Funding acquisition, Project administration, Writing – review & editing. **Olga Martín-Belloso:** Supervision, Funding acquisition, Project administration, Writing – review & editing. **Alan R. Mackie:** Conceptualization, Methodology, Visualization, Resources, Writing – review & editing, Supervision, Funding acquisition, Project administration.

Declaration of competing interest

The authors declare that they have no known competing financial interests or personal relationships that could have appeared to influence the work reported in this paper.

Data availability

Data will be made available on request.

Acknowledgements

This study was funded by the Ministry of Economy, Industry and Competitiveness (MINECO/FEDER, UE) throughout projects RTI2018-094268-B-C21 and AGL2015-65975-R. Anna Molet-Rodríguez thank the University of Lleida for their pre-doctoral fellow-ship and Campus iberus for the internship grant. Laura Salvia Trujillo thanks the 'Secretaria d'Universitats i Recerca del Departament d'Empresa i Coneixement de la Generalitat de Catalunya' for the Beatriu de Pinós post-doctoral grant (BdP2016 00336). The authors would like to acknowledge the support of N. Rigby for the pH-stat.

Appendix A. Supplementary data

Supplementary data related to this article can be found at https://doi.org/10.1016/j.foodhyd.2022.108121.

References

Boon, C. S., McClements, D. J., Weiss, J., & Decker, E. A. (2010). Factors influencing the chemical stability of carotenoids in foods. *Critical Reviews in Food Science and Nutrition, 50*(6), 515–532. https://doi.org/10.1080/10408390802565889

Brodkorb, A., Egger, L., Alminger, M., Alvito, P., Assunção, R., Ballance, S., et al. (2019). INFOGEST static in vitro simulation of gastrointestinal food digestion. *Nature Protocols, 14*(4), 991–1014. https://doi.org/10.1038/s41596-018-0119-1

Brummer, Y., Defelice, C., Wu, Y., Kwong, M., Wood, P. J., & Tosh, S. M. (2014). Textural and rheological properties of oat beta-glucan gels with varying molecular weight composition. *Journal of Agricultural and Food Chemistry, 62*(14), 3160–3167. https://doi.org/10.1021/jf405131d

Chuacharoen, T., & Sabliov, C. M. (2016). The potential of zein nanoparticles to protect entrapped b -carotene in the presence of milk under simulated gastrointestinal (GI) conditions. *LWT - Food Science and Technology, 72*, 302–309. https://doi.org/10.1016/j.lwt.2016.05.006

De Bont, P. W., Van Kempen, G. M. P., & Vreeker, R. (2002). Phase separation in milk protein and amylopectin mixtures. *Food Hydrocolloids, 16*(2), 127–138. https://doi.org/10.1016/S0268-005X(01)00070-4

Ferreira-Lazarte, A., Montilla, A., Mulet-Cabero, A. I., Rigby, N., Olano, A., Mackie, A., et al. (2017). Study on the digestion of milk with prebiotic carbohydrates in a simulated gastrointestinal model. *Journal of Functional Foods, 33*, 149–154. https://doi.org/10.1016/j.jff.2017.03.031

Fox, P. F., & Brodkorb, A. (2008). The casein micelle: Historical aspects, current concepts and significance. *International Dairy Journal, 18*(7), 677–684. https://doi.org/10.1016/j.idairyj.2008.03.002

Francis, M. J., Glover, Z. J., Yu, Q., Povey, M. J., & Holmes, M. J. (2019). Acoustic characterisation of pH dependant reversible micellar casein aggregation. *Colloids and Surfaces A: Physicochemical and Engineering Aspects, 568*, 259–265. https://doi.org/10.1016/j.colsurfa.2019.02.026

Gao, B., Luo, Y., Lu, W., Liu, J., Zhang, Y., & Yu, L. (2017). Triacylglycerol compositions of sunflower, corn and soybean oils examined with supercritical CO2 ultra-performance convergence chromatography combined with quadrupole time-of-flight mass spectrometry. *Food Chemistry, 218*, 569–574. https://doi.org/10.1016/j.foodchem.2016.09.099

Gasa-Falcon, A., Odriozola-Serrano, I., Oms-Oliu, G., & Martín-Belloso, O. (2017). Influence of Mandarin fiber addition on physico-chemical properties of nanoemulsions containing β-carotene under simulated gastrointestinal digestion conditions. *LWT - Food Science and Technology, 84*, 331–337. https://doi.org/10.1016/j.lwt.2017.05.070

Goh, K. K. T., Sarkar, A., & Singh, H. (2014). Milk protein–polysaccharide interactions. In B. Singh, & Thompson (Eds.), *Milk proteins* (2nd ed., pp. 387–419). Academic Press. https://doi.org/10.1016/b978-0-12-405171-3.00013-1.

Grundy, M. M. L., Quint, J., Rieder, A., Ballance, S., Dreiss, C. A., Cross, K. L., et al. (2017). The impact of oat structure and b-glucan on in vitro lipid digestion. *Journal of Functional Foods, 38*(A), 378–388. https://doi.org/10.1016/j.jff.2017.09.011

Jo, Y. J., & Kwon, Y. J. (2014). Characterization of β-carotene nanoemulsions prepared by microfluidization technique. *Food Science and Biotechnology, 23*(1), 107–113. https://doi.org/10.1007/s10068-014-0014-7

Karupaiah, T., & Sundram, K. (2007). Effects of stereospecific positioning of fatty acids in triacylglycerol structures in native and randomized fats: A review of their nutritional implications. *Nutrition and Metabolism, 4*(16), 1–17. https://doi.org/10.1186/1743-7075-4-16

Li, Y., Hu, M., & McClements, D. J. (2011). Factors affecting lipase digestibility of emulsified lipids using an in vitro digestion model: Proposal for a standardised pH-stat method. *Food Chemistry, 126*(2), 498–505. https://doi.org/10.1016/j.foodchem.2010.11.027

Li, Y., & McClements, D. J. (2010). New mathematical model for interpreting ph-stat digestion profiles: Impact of lipid droplet characteristics on in vitro digestibility. *Journal of Agricultural and Food Chemistry, 58*(13), 8085–8092. https://doi.org/10.1021/jf101325m

Liu, W., Wang, J., McClements, D. J., & Zou, L. (2018). Encapsulation of β-carotene-loaded oil droplets in caseinate/alginate microparticles: Enhancement of carotenoid stability and bioaccessibility. *Journal of Functional Foods, 40*, 527–535. https://doi.org/10.1016/j.jff.2017.11.046

Lubary, M., Hofland, G. W., & ter Horst, J. H. (2011). The potential of milk fat for the synthesis of valuable derivatives. *European Food Research and Technology, 232*(1), 1–8. https://doi.org/10.1007/s00217-010-1387-3

Mackie, A. R., Rafiee, H., Malcolm, P., Salt, L., & van Aken, G. (2013). Specific food structures supress appetite through reduced gastric emptying rate. *American Journal of Physiology - Gastrointestinal and Liver Physiology, 304*(11), 1038–1043. https://doi.org/10.1152/ajpgi.00060.2013

Maiani, G., Castón, M. J., Catasta, G., Toti, E., Cambrodón, I. G., Bysted, A., et al. (2009). Carotenoids: Actual knowledge on food sources, intakes, stability and bioavailability and their protective role in humans. *Molecular Nutrition & Food Research, 53*(2), S194–S218. https://doi.org/10.1002/mnfr.200800053

Mao, L., Xu, D., Yang, J., Yuan, F., Gao, Y., & Zhao, J. (2009). Effects of small and large molecule emulsifiers on the characteristics of β-carotene nanoemulsions prepared by high pressure homogenization. *Food Technology and Biotechnology, 47*(3), 336–342.

Mennah-Govela, Y. A., & Bornhorst, G. M. (2021). Food buffering capacity: Quantification methods and its importance in digestion and health. *Food & Function, 12*(2), 543–563. https://doi.org/10.1039/d0fo02415e

Mennah-Govela, Y. A., Singh, R. P., & Bornhorst, G. M. (2019). Buffering capacity of protein-based model food systems in the context of gastric digestion. *Food & Function, 10*(9), 6074–6087. https://doi.org/10.1039/c9fo01160a

Mulet-Cabero, A. I., Egger, L., Portmann, R., Ménard, O., Marze, S., Minekus, M., et al. (2020). A standardised semi-dynamic: In vitro digestion method suitable for food-an international consensus. *Food & Function, 11*(2), 1702–1720. https://doi.org/10.1039/c9fo01293a

Mulet-Cabero, A. I., Mackie, A. R., Wilde, P. J., Fenelon, M. A., & Brodkorb, A. (2019). Structural mechanism and kinetics of in vitro gastric digestion are affected by process-induced changes in bovine milk. *Food Hydrocolloids, 86*, 172–183. https://doi.org/10.1016/j.foodhyd.2018.03.035

Mulet-Cabero, A. I., Torcello-Gómez, A., Saha, S., Mackie, A. R., Wilde, P. J., & Brodkorb, A. (2020). Impact of caseins and whey proteins ratio and lipid content on in vitro digestion and ex vivo absorption. *Food Chemistry, 319*. https://doi.org/10.1016/j.foodchem.2020.126514, 126514.

Qian, C., Decker, E. A., Xiao, H., & McClements, D. J. (2012). Physical and chemical stability of β-carotene-enriched nanoemulsions: Influence of pH, ionic strength, temperature, and emulsifier type. *Food Chemistry, 132*(3), 1221–1229. https://doi.org/10.1016/j.foodchem.2011.11.091

Regand, A., Tosh, S. M., Wolever, T. M. S., & Wood, P. J. (2009). Physicochemical properties of glucan in differently processed oat foods influence glycemie response. *Journal of Agricultural and Food Chemistry, 57*(19), 8831–8838. https://doi.org/10.1021/jf901271v

Saini, R. K., Nile, S. H., & Park, S. W. (2015). Carotenoids from fruits and vegetables: Chemistry, analysis, occurrence, bioavailability and biological activities. *Food Research International journal, 76*, 735–750. https://doi.org/10.1016/j.foodres.2015.07.047

Salaün, F., Mietton, B., & Gaucheron, F. (2005). Buffering capacity of dairy products. *International Dairy Journal, 15*(2), 95–109. https://doi.org/10.1016/j.idairyj.2004.06.007

Salvia-Trujillo, L., Qian, C., Martín-Belloso, O., & McClements, D. J. (2013). Modulating β-carotene bioaccessibility by controlling oil composition and concentration in edible nanoemulsions. *Food Chemistry, 139*(1–4), 878–884. https://doi.org/10.1016/j.foodchem.2013.02.024

Sarantis, S. D., Eren, N. M., Kowalcyk, B., Jimenez–Flores, R., & Alvarez, V. B. (2021). Thermodynamic interactions of micellar casein and oat β-glucan in a model food system. *Food Hydrocolloids, 115*. https://doi.org/10.1016/j.foodhyd.2020.106559, 106559.

Sun, C., Gunasekaran, S., & Richards, M. P. (2007). Effect of xanthan gum on physicochemical properties of whey protein isolate stabilized oil-in-water emulsions. *Food Hydrocolloids, 21*(4), 555–564. https://doi.org/10.1016/j.foodhyd.2006.06.003

Tam, J. J., & Whitaker, J. R. (1972). Rates and extents of hydrolysis of several caseins by pepsin, rennin, endothia parasitica protease and mucor pusillus protease. *Journal of Dairy Science, 55*(11), 1523–1531. https://doi.org/10.3168/jds.S0022-0302(72)85714-X

Thomas, A. (2006). Gut motility, sphincters and reflex control. *Anaesthesia and Intensive Care Medicine, 7*(2), 57–58. https://doi.org/10.1383/anes.2006.7.2.57

Thongngam, M., & McClements, D. J. (2005). Isothermal titration calorimetry study of the interactions between chitosan and a bile salt (sodium taurocholate). *Food Hydrocolloids, 19*(5), 813–819. https://doi.org/10.1016/j.foodhyd.2004.11.001

Timm-Heinrich, M., Xu, X., Nielsen, N. S., & Jacobsen, C. (2003). Oxidative stability of structured lipids produced from sunflower oil and caprylic acid. *European Journal of Lipid Science and Technology, 105*(8), 436–448. https://doi.org/10.1002/ejlt.200300794

Tosh, S. M., Brummer, Y., Wood, P. J., Wang, Q., & Weisz, J. (2004). Evaluation of structure in the formation of gels by structurally diverse (1 → 3)(1 → 4)-β-D-glucans from four cereal and one lichen species. *Carbohydrate Polymers, 57*(3), 249–259. https://doi.org/10.1016/j.carbpol.2004.05.009

Verkempinck, S. H. E., Salvia-Trujillo, L., Moens, L. G., Charleer, L., Van Loey, A. M., Hendrickx, M. E., et al. (2018). Emulsion stability during gastrointestinal conditions effects lipid digestion kinetics. *Food Chemistry, 246*, 179–191. https://doi.org/10.1016/j.foodchem.2017.11.001

White, D. A., Fisk, I. D., & Gray, D. A. (2006). Characterisation of oat (Avena sativa L.) oil bodies and intrinsically associated E-vitamers. *Journal of Cereal Science, 43*(2), 244–249. https://doi.org/10.1016/j.jcs.2005.10.002

Wu, J., Zhang, Y., Wang, L., Xie, B., Wang, H., & Deng, S. (2006). Visualization of single and aggregated hulless oat (avena nuda L.) (1→3),(1→4)-β- d -glucan molecules by atomic force microscopy and confocal scanning laser microscopy. *Journal of Agricultural and Food Chemistry, 54*(3), 925–934. https://doi.org/10.1021/jf0523059

Zhang, R., Zhang, Z., Zou, L., Xiao, H., Zhang, G., Decker, E. A., et al. (2016). Enhancement of carotenoid bioaccessibility from carrots using excipient emulsions: Influence of particle size of digestible lipid droplets. *Food & Function, 7*(1), 93–103. https://doi.org/10.1039/C5FO01172H